https://doi.org/10.2352/ISSN.2470-1173.2019.13.COIMG-134

Distance Retrieval from Unknown View Tomography of 2D Point Sources

Mona Zehni, Shuai Huang, Ivan Dokmanić, Zhizhen Zhao
Coordinated Science Laboratory, University of Illinois at Urbana-Champaign, Champaign, IL

Abstract

In this paper, we study a 2D tomography problem with random and unknown projection angles for a point source model. Specifically, we target recovering geometry information, i.e. the radial and pairwise distances of the underlying point source model. For this purpose, we introduce a set of rotation-invariant features that are estimated from the projection data. We further show these features are functions of the radial and pairwise distances of the point source model. By extracting the distances from the features, we gain insight into the geometry of the unknown point source model. This geometry information can be used later on to reconstruct the point source model. The simulation results verify the robustness of our method in presence of noise and errors in the estimation of the features.

Introduction

Let us consider the forward model as,

$$s_\ell[u] = \mathscr{D}\{\mathscr{P}_{\theta_\ell} I\}[u] + \varepsilon_\ell[u], \quad \ell \in \{1,2,...,L\}$$
$$I(x,y) = \sum_{k=1}^{K} \delta(x-x_k, y-y_k) \tag{1}$$

where I is the point source model and s_ℓ is the ℓ-th projection line in a projection set of size L. I consists of K Dirac deltas located at $\{(x_k,y_k)\}_{k=1}^K \in \mathbb{R}^2$. Here for the sake of simplicity, we assume unit equal weights for all the point sources. $\mathscr{P}_\theta$ is the radon transform operator along θ direction and θ marks the angle between the projection direction and the horizontal axis. We assume θ_ℓ to be drawn uniformly from $[0,2\pi)$. In order to account for the finite resolution of the measurements, $\mathscr{D}$ is introduced which samples $\mathscr{P}_{\theta_\ell} I$ every Δ as,

$$\mathscr{D}(f)[u] = \int_{(u-\frac{1}{2})\Delta}^{(u+\frac{1}{2})\Delta} f(x)dx, \text{ for } u \in \{-M,\dots,M\}, \tag{2}$$

where larger M leads to higher resolution in measuring the projection line. Finally, the digitized projections are contaminated by Gaussian noise with zero mean and σ^2 variance, i.e. $\varepsilon_\ell[u] \sim \mathscr{N}(0,\sigma^2)$.

Let $r_k = \sqrt{x_k^2+y_k^2}$, $\forall k \in \{1,2,...,K\}$ denote the radial distance between the k-th point source and the origin. Also, $d_{m,n} = \sqrt{(x_m-x_n)^2+(y_m-y_n)^2}$, $\forall m,n \in \{1,2,...,K\}$, is the pairwise distance between m-th and n-th point sources. In this paper, our target is to recover the radial $\{r_k\}_{k=1}^K$ and pairwise distances $\{d_{m,n}\}_{m,n=1}^K$ from the projection data $\{s_\ell\}_{\ell=1}^L$. This work is based on our paper [1] which provides a detailed discussion on how the point source model is recovered from distance distributions following [2].

Recovering an unknown point-source model from a set of measurements emerges in many fields such as array signal processing [3], super-resolution [4], compressed sensing [5], radio astronomy [6]-[7], unassigned distance geometry [8]-[9], X-ray crystallography [10] and cryo-electron microscopy atomic modeling [11], to name a few. For the set of measurements provided by the forward model (1), a classical approach to recover I is to formulate the problem as a sparse 2D tomography problem [13]-[14]. However, this method relies on the knowledge of the projection angles $\{\theta_\ell\}_{\ell=1}^L$ which is not available in our problem setting.

In this paper, we aim at extracting the radial and pairwise distances of the point-source model. For this purpose, we introduce a set of rotation-invariant features that are estimated from the projection data. These features are informative of the geometry of the underlying point source model and their estimation does not require the knowledge of the projection angles. In addition, these features are expressed as summations of zeroth-order Bessel function of the first kind and they are functions of $\{r_k\}_{k=1}^K$ and $\{d_{m,n}\}_{m,n=1}^K$. Using the asymptotic behavior of Bessel functions, the distance recovery is posed as a harmonic retrieval problem and solved by forward-backward Prony's method. Our simulation results verify the robustness of our method to noise when sufficient number of projection lines are available.

Method

In this section we describe the estimation of the rotation-invariant features from the projection lines. Subsequently, we propose a method to extract the radial and pairwise distances from the features.

Estimating the rotation-invariant features

In our problem, we have access to a large number of projection data $\{s_\ell\}_{\ell=1}^L$. This enables us to derive features that reflect the geometry of the underlying point-source model. In our point-source model, all point sources are compactly supported by a disk of radius R and the center of mass is located at origin. Following the definition of radon transform as line integrals, we have

$$(\mathscr{P}_\theta I)(r) = \sum_{k=1}^{K} \delta(r-(y_k\cos\theta - x_k\sin\theta)). \tag{3}$$

This shows that the radon transform of a point-source signal consists of Dirac deltas translated according to the projection angle

This work is partially supported by National Science Foundation under Grant CIF-1817577.

θ. To account for the finite resolution of the detected projection line, we apply the $\mathscr{D}$ operator defined in (2) to (3) as,

$$g_\theta[u] = (\mathscr{D}\mathscr{P}_\theta I)[u] = \sum_{k=1}^{K} \mathbf{1}_{\frac{y_k\cos\theta - x_k\sin\theta}{\Delta} \in [u-\frac{1}{2}, u+\frac{1}{2}]}, \tag{4}$$

where $u \in \{-M,\dots,M\}$, $\mathbf{1}_{\mathscr{C}} = 1$ if condition $\mathscr{C}$ is satisfied and $\mathbf{1}_{\mathscr{C}} = 0$ otherwise. Note that as the point sources lie within a disk of radius R, each projection line is compactly supported in $[-R,R]$ interval. Then, sampling $\mathscr{P}_\theta I$ with $\mathscr{D}$ operator implies that the support of length $2R$ is divided into $2M+1$ bins, i.e. $\Delta = \frac{2R}{2M+1}$.

To derive the rotation-invariant features, let us first derive the discrete Fourier transform (DFT) of the projection lines as,

$$\hat{g}_\theta[v] = \sum_{k=1}^{K} \exp\left(\imath \tfrac{2\pi v}{(2M+1)} \left\lfloor \tfrac{y_k\cos\theta - x_k\sin\theta}{\Delta} \right\rceil\right), \tag{5}$$

where $\lfloor x \rceil$ denotes the closest integer to x. If Δ is small enough (equivalently if M is large enough), then $\left\lfloor \frac{y_k\cos\theta - x_k\sin\theta}{\Delta} \right\rceil \approx \frac{y_k\cos\theta - x_k\sin\theta}{\Delta}$. Following this approximation, the first rotation-invariant features is defined as,

$$\begin{aligned}
\mu[v] &= \mathbb{E}_\theta\{\hat{g}_\theta[v]\} \\
&= \sum_{k=1}^{K} \mathbb{E}_\theta\left\{\exp\left(\imath \frac{2\pi}{2M+1} \frac{y_k\cos\theta - x_k\sin\theta}{\Delta} v\right)\right\} \\
&\overset{(a)}{=} \sum_{k=1}^{K} \frac{1}{2\pi} \int_0^{2\pi} \exp\left(\imath \frac{2\pi}{2M+1} \frac{y_k\cos\theta - x_k\sin\theta}{\Delta} v\right) d\theta \\
&\overset{(b)}{=} \sum_{k=1}^{K} J_0\left(\frac{\pi r_k}{R} v\right)
\end{aligned} \tag{6}$$

where (a) is a consequence of $\theta \sim \text{Unif}[0,2\pi)$ and (b) is based on the integral defined in [12]. Also, $J_0(\cdot)$ is the zeroth order Bessel function of the first kind.

Following the same steps, we have,

$$\begin{aligned}
\mathbb{E}_\theta\{|\hat{g}_\theta[v]|^2\} &\approx \sum_{m=1}^{K}\sum_{n=1}^{K} J_0\left(\frac{\pi d_{m,n}}{R} v\right) \\
&= K J_0(0) + 2\sum_{m=1}^{K}\sum_{n=m+1}^{K} J_0\left(\frac{\pi d_{m,n}}{R} v\right).
\end{aligned} \tag{7}$$

Hence, the second rotation-invariant feature is defined as,

$$C[v] = \left(\mathbb{E}_\theta\left\{|\hat{g}_\theta[v]|^2\right\} - K\right)/2. \tag{8}$$

The radial and pairwise distances are invariant to global rotations of the point source model, so are the features defined in (6) and (8), hence the name rotation-invariant.

To estimate the rotation-invariant features, we use the projection data $\{s_\ell\}_{\ell=1}^{L}$ as,

$$\widehat{\mu}[v] = \frac{1}{L}\sum_{\ell=1}^{L} \widehat{s}_\ell[v], \tag{9}$$

$$\widehat{C}[v] = \left(\frac{1}{L}\sum_{\ell=1}^{L} |\widehat{s}_\ell[v]|^2 - (2M+1)\sigma^2 - K\right)/2, \tag{10}$$

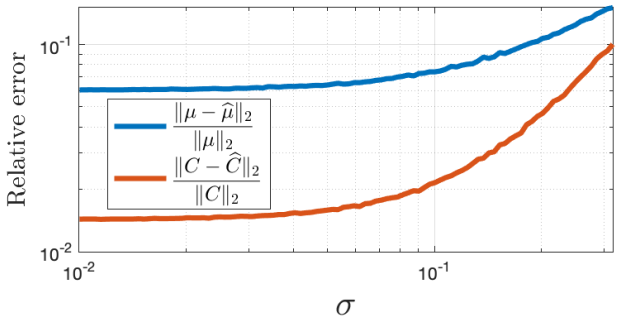

Fig. 1. *Relative error in estimating the rotation-invariant features from the projection data versus standard deviation of noise.*

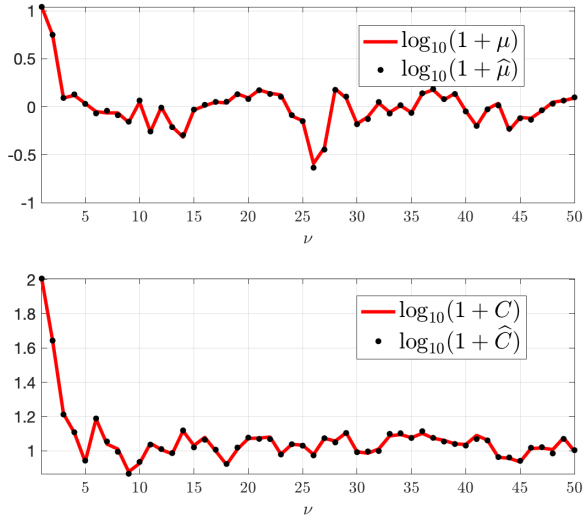

Fig. 2. *Comparison between the estimated features in* (9)-(10) *and their analytical expressions in* (6)-(8) *for a randomly generated point source model with* $K = 10$ *and* $SNR = 1$.

where $\widehat{s}_\ell[v]$ is an empirical realization of $\hat{g}_\theta[v]$ and is obtained by taking FFT of s_ℓ. Also, subtracting $(2M+1)\sigma^2$ in (10) serves to debias the estimation of C. By the law of large numbers, the sample estimates $\widehat{\mu}$ and $\widehat{C}$ converge to μ and C when the sample size $L \to \infty$. The relative error between the estimated features and their analytical expressions versus σ is plotted in Fig. 1. This plot implies that for small values of σ, $\frac{\|\mu-\widehat{\mu}\|_2}{\|\mu\|_2}$ and $\frac{\|C-\widehat{C}\|_2}{\|C\|_2}$ is almost constant. The feature estimation error in the low-noise regimes originates from the approximations made earlier. On the other hand, for larger values of σ, the relative error in estimating C grows more rapidly compared to μ. For higher noise regimes, more projection samples are required in order to estimate the features accurately. In fact, the sample size for accurate estimation of μ and C grows with $O(\sigma^2)$ and $O(\sigma^4)$ respectively. In addition, a schematic of μ and C alongside their estimations for a point-source model example is provided in Fig. 2. Note that *SNR* refers to the average signal to noise ratio of the projection lines $\{s_\ell\}_{\ell=1}^{L}$ and is defined as $SNR = \frac{K}{(2M+1)\sigma^2}$.

Algorithm 1 Extracting radial and pairwise distances from invariant features

Input: Projection data, $\{s_\ell\}_{\ell=1}^{L}$
Output: The estimated $\{r_k,\}_{k=1}^{K}, \{d_{m,n}\}_{m,n=1}^{K}$.

1: Estimate the rotation invariant features, $\widehat{\mu}$ and $\widehat{C}$ using (9)-(10).
2: Apply Prony's method to extract $\{r_k,\}_{k=1}^{K}$ and $\{d_{m,n}\}_{m,n=1}^{K}$.

Recovering the geometry information of the model

We now focus on extracting the geometry information of the model, i.e. $\{r_k\}_{k=1}^{K}$ and $\{d_{m,n}\}_{m,n=1}^{K}$, from the features estimated in (9)-(10). For this purpose, we make use of the asymptotic behaviour of the Bessel function [12, p.364] as,

$$J_0(z) \approx \sqrt{\frac{2}{\pi z}} \cos\left(z - \frac{\pi}{4}\right), \tag{11}$$

for $z \gg 1/4$. Substituting (11) in (6) and (8) leads to,

$$\widehat{\mu}[\nu] \approx \sum_{k=1}^{K} \frac{e^{\imath\left(a_k\nu - \pi/4\right)} + e^{-\imath\left(a_k\nu - \pi/4\right)}}{\sqrt{2\pi a_k \nu}}, \tag{12}$$

$$\widehat{C}[\nu] \approx \sum_{m=1}^{K} \sum_{n=m+1}^{K} \frac{e^{\imath\left(b_{m,n}\nu - \pi/4\right)} + e^{-\imath\left(b_{m,n}\nu - \pi/4\right)}}{\sqrt{2\pi b_{m,n} \nu}} \tag{13}$$

where $a_k = \frac{\pi r_k}{R}$ and $b_{m,n} = \frac{\pi d_{m,n}}{R}$, for an integer $\nu \gg \max_k \lceil \frac{1}{4a_k} \rceil$ and $\nu \gg \max_{m,n} \lceil \frac{1}{4d_{m,n}} \rceil$. After scaling (12)-(13) by $\sqrt{\nu}$, the new features $\sqrt{\nu}\widehat{\mu}$ and $\sqrt{\nu}\widehat{C}$ are weighted summations of complex exponentials. Now, extracting $\{r_k\}_{k=1}^{K}$ and $\{d_{m,n}\}_{m,n=1}^{K}$ is translated as retrieving the harmonics of the new features. For this purpose, we use Prony's method which is briefly reviewed afterwards. Our procedure for extracting the radial and pairwise distances is outlined in Alg. 1.

Prony's method

Prony's method and its variants are widely used in harmonic retrieval literature [15]. Imagine a discrete signal w which is a weighted summation of complex exponentials as follows,

$$w[m] = \sum_{k=1}^{K} \alpha_k e^{-\jmath t_k m}, \quad m \in \mathbb{Z} \tag{14}$$

where t_k and α_k, $k \in \{1,...,K\}$, mark the k-th harmonic and weight respectively, and K is the total number of complex exponentials with distinct harmonics. In a harmonic retrieval problem, the measurements are samples of w (probably contaminated by noise). However, the harmonics $\{t_k\}_{k=1}^{K}$ and the weights $\{\alpha_k\}_{k=1}^{K}$ are unknown and the goal is to recover them from w.

Note that (14) suggests that w is a solution of a discrete differential equation written as,

$$w[m] + b_1 w[m-1] + b_2 w[m-2] + ... + b_K w[m-K] = 0, \tag{15}$$

where $\{b_k\}_{k=1}^{K}$ are the weights of the differential equation. Taking Z-transform of (15) leads to,

$$b_1 z^{-1} + b_2 z^{-2} + ... + b_K z^{-K} = -1. \tag{16}$$

Note that for known $\{b_k\}_{k=1}^{K}$, the roots of (16) are $\{e^{-\jmath t_k}\}_{k=1}^{K}$. Thus, the first step in Prony's method is to find the weights of the differential equation in (16), i.e. $\{b_k\}_{k=1}^{K}$. By stacking $N-K$ equations as in (15), we have,

$$\begin{bmatrix} w[K-1] & w[K-2] & \cdots & w[0] \\ w[K] & w[K-1] & \cdots & w[1] \\ w[K+1] & w[K] & \cdots & w[2] \\ \vdots & \vdots & \cdots & \vdots \\ w[N-2] & w[N-3] & \cdots & w[N-K] \end{bmatrix} \begin{bmatrix} b_1 \\ b_2 \\ b_3 \\ \vdots \\ b_K \end{bmatrix} = - \begin{bmatrix} w[K] \\ w[K+1] \\ w[K+2] \\ \vdots \\ w[N-1] \end{bmatrix} \tag{17}$$

where $N \geq 2K$. Next, we solve (17) to derive $\{b_k\}_{k=1}^{K}$ and find the roots for (16) accordingly.

In general, there is no guarantee that the roots derived from (16) are all complex exponentials. To further impose this constraint, one can argue if g is a complex exponential root of (16), so is $\overline{g}^{-1}$, where $\overline{g}$ is the complex conjugate of g. Note that this constraint on the roots is not exactly the same as enforcing them to be complex exponentials. However, it is still helpful in further narrowing down the roots toward being complex exponentials (especially for noisy observations). Hence, it is possible to augment (17) with more equations based on this constraint which leads to,

$$\begin{bmatrix} w[K-1] & w[K-2] & \cdots & w[0] \\ w[K] & w[K-1] & \cdots & w[1] \\ w[K+1] & w[K] & \cdots & w[2] \\ \vdots & \vdots & \cdots & \vdots \\ w[N-2] & w[N-3] & \cdots & w[N-K] \\ \overline{w}[1] & \overline{w}[2] & \cdots & \overline{w}[K] \\ \overline{w}[2] & \overline{w}[3] & \cdots & \overline{w}[K+1] \\ \vdots & \vdots & \cdots & \vdots \\ \overline{w}[N-K] & \overline{w}[N-K+1] & \cdots & \overline{w}[N-1] \end{bmatrix} \begin{bmatrix} b_1 \\ b_2 \\ b_3 \\ \vdots \\ b_K \end{bmatrix} = - \begin{bmatrix} w[K] \\ w[K+1] \\ w[K+2] \\ \vdots \\ w[N-1] \\ \overline{w}[0] \\ \vdots \\ \overline{w}[N-K-1] \end{bmatrix} \tag{18}$$

Solving (18) for $\{b_k\}_{k=1}^{K}$ and finding the roots of (16) is called forward-backward Prony's method. We use this method in order to extract $\{r_k\}_{k=1}^{K}$ and $\{d_{m,n}\}_{m,n=1}^{K}$ from samples of $\sqrt{\nu}\widehat{\mu}$ and $\sqrt{\nu}\widehat{C}$ in (12)-(13). Note that some recovered roots might not lie on the unit circle in the complex plain. Thus, to achieve the final complex exponentials, we project the recovered roots on the unit circle by taking their phase. It is worth mentioning that after deriving $\{t_k\}_{k=1}^{K}$, the weights are recovered by solving a system of linear equations.

Experiments

We generate point source models by generating K points uniformly distributed in $[-1,1] \times [-1,1]$ support. Note that we impose a minimum distance separation between the points as $\min_{i,j \in \{1,...,K\}, i \neq j} |r_i - r_j| \geq 0.1$. Next we generate $L = 10^4$ projection lines following (1). Note that the projection angle corresponding to each projection line is drawn from a uniform distribution over $[0, 2\pi)$ interval. Finally, Gaussian noise with zero mean and σ^2 variance is added to the clean digitized projection lines.

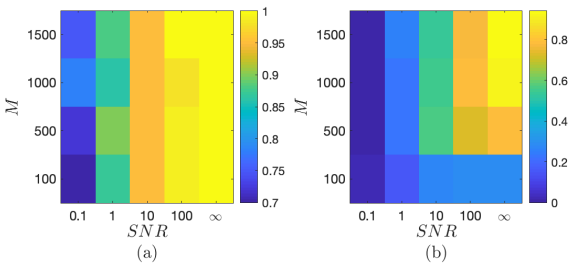

Fig. 3. *Successful recovery rate for (a) the radial distance distribution, (b) the pairwise distance distribution.*

In order to evaluate the performance of Alg. (1) in recovering the radial and pairwise distances, we use earth mover's distance (EMD) metric [16]. EMD is mainly used to find the distance between two probability distributions. Thus, using EMD we measure the distances between the ground truth and recovered radial and pairwise distances. A recovery is successful if the EMD between the ground truth and the recovered distribution is less than $th = 0.1$. To define the success rate of recovery, we generate $N = 100$ random realizations as point-source models. Then, the ratio of the successfully recovered distance (radial and pairwise) represents success rate of recovery.

Figure 3 demonstrates the success recovery rates for (a) radial, (b) pairwise distances. These results convey,

- Smaller M leads to lower resolution in measuring the projection lines, which in turn leads to lower success rate of recovery. However, when M is sufficiently large ($M \geq 500$), increasing M does not affect the success recovery rate significantly.
- As SNR increases, the success recovery rate improves. Note that $SNR = \infty$ refers to the no noise regime.
- Comparing (a) and (b) shows that success rate for recovering the pairwise distances is lower compared to the radial distances. This is due to the fact that for $K = 5$, there are 5 radial and 10 pairwise distances. As a result, recovering the pairwise distances require retrieving more harmonics compared to the radial distances.

Conclusion

In this paper we studied the problem of recovering a point source model from a set of projection lines whose projection angles were random and unknown. Extracting geometry information of the underlying point-source model takes us one step closer to the reconstruction of the point-source model. In order to obtain geometric information about the underlying source model, we aimed at recovering the radial and pairwise distances. We tackled this problem by introducing a set of rotation-invariant features that were estimated based on the projection data. We showed that these features reveal the radial and pairwise distances and they are expressed in forms of summations of Bessel functions of the first kind and zeroth-order. Next, we leveraged from the asymptotic behavior of the Bessel functions and used Prony's method in order to extract the distances. Through our simulation results we showed the robustness of our method in different noise levels when sufficient number of projection samples are available.

References

[1] M. Zehni, S. Huang, I. Dokmanić and Z. Zhao, Geometric Invariants for Sparse Unknown View Tomography, ArXiv e-prints, (2018).

[2] S. Huang and I. Dokmanić, Reconstructing Point Sets from Distance Distributions, ArXiv e-prints, (2018).

[3] H. Krim and M. Viberg, Two decades of array signal process-ing research: the parametric approach, IEEE Signal Process-ing Magazine, 13, 4 (1996).

[4] E. J. Candés and C. Fernandez-Granda, Towards a mathematical theory of super-resolution, Communications on Pure and Applied Mathematics, 67, 6 (2014).

[5] H. Boche, R. Calderbank, G. Kutyniok, and J. Vybíral, A Survey of Compressed Sensing, Springer International Publishing, (2015).

[6] H. Pan, T. Blu, and M. Vetterli, Towards generalized FRI sampling with an application to source resolution in radio astronomy, IEEE Transactions on Signal Processing, 65, 4 (2017).

[7] H. Pan, M. Simeoni, P. Hurley, T. Blu, and M. Vetterli, LEAP:Looking beyond pixels with continuous-space EstimAtion of Point sources, Astronomy and Astrophysics, 608, (2017).

[8] S. J. L. Billinge, P. M. Duxbury, D. S. Gonçalves, C. Lavor, and A. Mucherino, Assigned and unassigned distance geometry:applications to biological molecules and nanostructures, 4OR, 14, 4 (2016).

[9] P. Duxbury, L. Granlund, S. Gujarathi, P. Juhas, and S. Billinge, The unassigned distance geometry problem, Dis-crete Appl. Math., 204, 11 (2016).

[10] D. Jan and J. Mesters, Principles of Protein X-Ray Crystallography, Springer, New York, (2007).

[11] F. Gramm, C. Baerlocher, L. B. McCusker, S. J. Warrender, P. A. Wright, B. Han, S. B. Hong, Z. Liu, T. Ohsuna, and O. Terasaki, Complex zeolite structure solved by combining powder diffraction and electron microscopy, Nature, 444, (2006).

[12] M. Abramowitz and I. A. Stegun, Handbook of Mathematical Functions with Formulas, Graphs, and Mathematical Tables, Dover, 1972, pg. 358–364.

[13] L. Stanković and M. Daković, On a Gradient-Based Algorithm for Sparse Signal Reconstruction in the Signal/Measurements Domain, Mathematical Problems in Engineering, 2016, (2016).

[14] Y. Kaganovsky, D. Li, A. Holmgren, H. Jeon, K. P. MacCabe, D. G. Politte, J. A. O'Sullivan, L. Carin, and D. J. Brady, Compressed sampling strategies for tomography, J. Opt. Soc. Am. A 31, (2014).

[15] L. Weiss, and R. N. McDonough. Prony's method, Z-transforms, and Padé approximation. SIAM Review, 5, 2 (1963).

[16] Y. Rubner, C. Tomasi, L. J. Guibas, The Earth Mover's Distance as a Metric for Image Retrieval, International J. of Computer Vision, 40, 2 (2000).

JOIN US AT THE NEXT EI!

IS&T International Symposium on

Electronic Imaging

SCIENCE AND TECHNOLOGY

Imaging across applications . . . Where industry and academia meet!

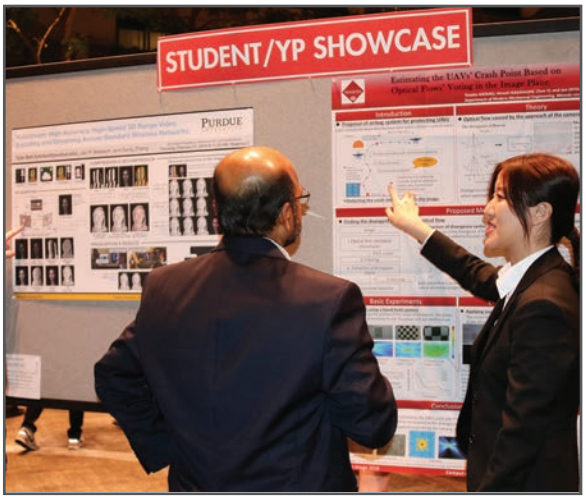

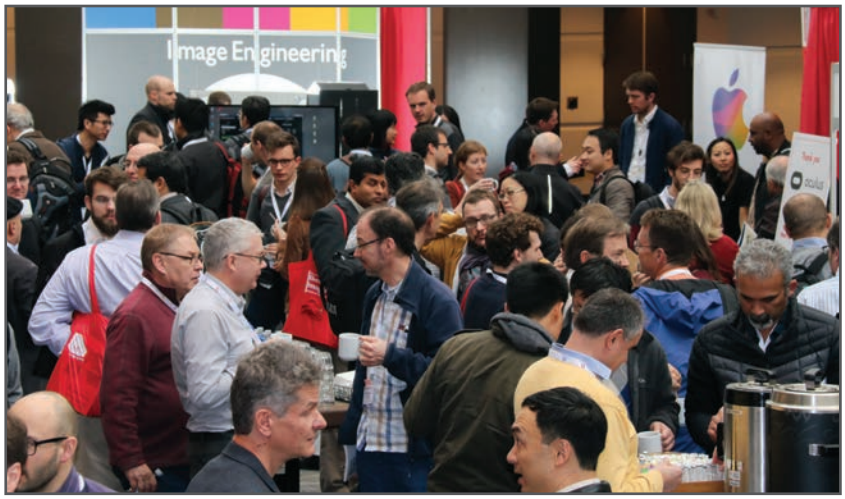

• SHORT COURSES • EXHIBITS • DEMONSTRATION SESSION • PLENARY TALKS •
• INTERACTIVE PAPER SESSION • SPECIAL EVENTS • TECHNICAL SESSIONS •

www.electronicimaging.org

IS&T
imaging.org